

Electronic Supplementary Information

Crystallisation Temperature Control of Stoichiometry and Selectivity in Host-Guest Compounds

Nicole M. Sykes, Hong Su, Edwin Weber, Susan A. Bourne and Luigi R. Nassimbeni

Table of Contents

1. Methods and Materials.....	1
2. X-ray Crystallography	1
3. ¹ H Nuclear Magnetic Resonance (NMR) Spectroscopy	2
4. Hydrogen Bonding	3
5. Structure diagrams	4
6. Apohost Composition	5
7. Packing comparisons between structures 1, 3 and 6	6
8. Lattice Energy	7
9. Representative Inclusion Experiments	8
10. Hirshfeld Analysis.....	18
11. Kinetics of <i>In Situ</i> PXRD Vapour Sorption (Experiment 1).....	23
12. Relevant Thermal Analysis.....	23

1. Materials and Methods

The host compound 9,9'-(ethyne-1,2-diyl)bis(fluoren-9-ol), **H** was synthesized by Weber¹ and used without further purification. The alcohol guests were purchased from Sigma Aldrich and used as received. Single crystals of the inclusion compounds were obtained by dissolving **H** in chloroform and adding an excess of the guest or binary guest mixture. The resulting solutions were filtered and allowed to crystallise at various temperatures. Heating mantles were used to achieve the temperatures of +30°C and +50 and vials were left open to slowly evaporate. This is acceptable given that the vapour pressures of the two guests are so similar; at 20°C the vapour pressure of 2-propanol is 4.24 kPa and that of tertiary butanol is 3.98 kPa. At the lower temperatures vials were capped and sealed with parafilm; +5°C and -20°C were realised by using a standard fridge and freezer. The low temperatures of -41°C and -61°C were achieved by allowing solutions to crystallise in a slurry of acetonitrile/dry ice and chloroform/dry ice respectively.

2. X-ray Crystallography

Single crystal X-ray diffraction data were collected on a Bruker DUO APEX II² diffractometer for all structures using Mo K α ($\lambda = 0.71073 \text{ \AA}$) at a temperature of 153 K. The intensity data were collected using the phi scan and omega scan techniques, scaled and reduced with

SAINT-Plus.³ The correction of the collected intensities for absorption was done using the SADABS program.⁴

The structures were solved by direct methods using SHELX-97⁵ and refined using full-matrix least squares methods in SHELXL.⁵ The graphical interface used was the program X-SEED.⁶ All C-H hydrogen atoms were placed geometrically and with a riding model for their isotropic temperature factors. The O-H hydrogen atoms were located in the final difference electron density map. Their bond lengths were fixed using the formulae suggested by Lusi and Barbour⁷ who studied the neutron data of the O-H...O systems. Diagrams were generated using MERCURY (3.9).⁸

Powders were mounted on a flat zero-background sample holder. X-ray powder data were collected in a Bruker D8 Advance X-ray diffractometer with copper radiation (Cu K α , λ = 1.5406 Å) at 30 kV and 40 mA. Each sample was scanned between 4 and 32° 2 θ with a step size of 0.02°.

3. ¹H Nuclear Magnetic Resonance (NMR) Spectroscopy

¹H NMR spectra were recorded on a Bruker 300MHz with DMSO as internal standard. Samples were blotted dry, crushed, and dissolved in deuterated d6-DMSO. The appropriate CH₃ signals were integrated to determine the relative proportions of the guests.

References

- (1) E. Weber, S. Nitsche, A. Wierig, I. Csöreg. *Eur. J. Org. Chem.* 2002, **5**, 856.
- (2) APEX 2, Version 1.0-27; Bruker AXS Inc.; Madison, WI, 2005.
- (3) SAINT-Plus, Version 7.12; Bruker AXS Inc.: Madison, Wisconsin, USA, 2004.
- (4) G. M. Sheldrick. SADABS: Program for Area Detector Adsorption Correction; University of Göttingen: Germany, 1997; p. 33.
- (5) G. M. Sheldrick SHELX-97: Program for Crystal Structure Solution and Refinement; University of Göttingen: Germany, 1997; p. 1456.
- (6) L. J. Barbour. *J. Supramol. Chem.* 2001, **1**, 189.
- (7) M. Lusi, L. J. Barbour. *Cryst. Growth Des.*, 2011, **11**, 5515.
- (8) C. F. Macrae, I. J. Bruno, J. A. Chisholm, P. R. Edgington, P. McCabe, E. Pidcock, L. Rodriguez-Monge, R. Taylor, J. Van de Streek, P. A. Wood. Mercury CSD 3.5.1. New Features for the Visualization and Investigation of Crystal Structures. *J. Appl. Crystallogr.* 2008, **41**, 466.

4. Hydrogen bonding

Table 2. Hydrogen bonding.

Compound	Donor (O)	Acceptor (O)	O...O (Å)	O-H(Å)	O...A (Å)	<O-H...O(°)
1	O16	O41	2.743(2)	0.967(5)	1.785(7)	171(2)
	O41	O95	2.707(2)	0.979(5)	1.729(6)	177(3)
	O95	O13	2.761(2)	0.969(5)	1.829(10)	161(2)
	O13	O92	2.753(2)	0.966(5)	1.787(5)	179(3)
	O92	O16 ^a	2.931(2)	0.946(5)	2.080(15)	149(2)
	O89	O69	2.891(2)	0.955(5)	2.033(18)	148(3)
	O69	O44	2.726(2)	0.968(5)	1.770(7)	169(2)
	O44	O86	2.646(2)	0.989(5)	1.663(7)	172(3)
	O86	O72	2.744(2)	0.969(5)	1.812(11)	160(3)
	O72	O89 ^b	2.768(2)	0.970(5)	1.802(7)	173(3)
2	O16	O13	2.770(2)	0.965(5)	1.825(8)	165(2)
	O13	O16 ^c	2.668(2)	0.971(5)	1.745(9)	158(2)
3	O16	O41	2.739(2)	0.964(5)	1.781(6)	171(2)
	O41	O44	2.689(2)	0.978(5)	1.713(6)	176(2)
	O44	O13	2.766(2)	0.967(5)	1.817(7)	166(2)
	O13	O48	2.753(2)	0.964(5)	1.792(6)	175(2)
	O48	O16 ^a	2.885(2)	0.948(5)	2.03(15)	148(2)
4	O13	O20	2.680(2)	0.977(5)	1.706(6)	175(2)
	O20	O16	2.706(2)	0.977(5)	1.736(6)	171(2)
	O16	O13 ^d	2.781(2)	0.967(5)	1.816(6)	176(2)
5	O13	O62	2.674(2)	0.976(5)	1.698(5)	178(2)
	O62	O41	2.834(1)	0.945(5)	1.895(6)	172(2)
	O41	O16	2.723(2)	0.963(5)	1.761(5)	177(2)
	O16	O65	2.753(2)	0.964(5)	1.799(7)	169(2)
	O65	O44	2.853(2)	0.946(5)	1.913(6)	172(2)
	O44	O59	2.674(2)	0.973(5)	1.701(5)	176(2)
	O59	O13 ^e	2.719(2)	0.964(5)	1.759(6)	174(2)
6	O16	O47	2.704(2)	0.964(5)	1.748(5)	171(2)
	O47	O41	2.753(2)	0.968(5)	1.790(6)	174(2)
	O41	O43	2.672(2)	0.975(5)	1.723(8)	163(2)
	O43	O13	2.814(2)	0.954(5)	1.869(9)	171(4)

Symmetry codes: (a) 1-x, 1-y, -z (a) x-1, y, z (b) x+1, y, z (c) 1-x, -y, 1-z (d) -x, 1-y, -z (e) x, y-1, z

5. Structure diagrams

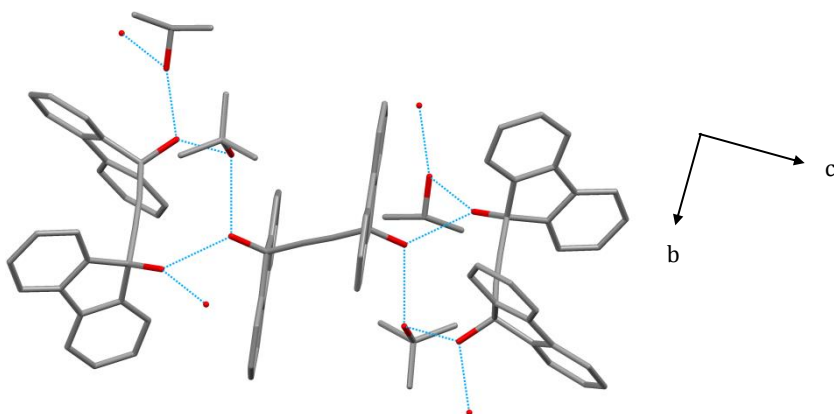


Figure 5.1: Structure **3**, grown at 50°C from an equimolar guest mixture of **2-PROP** and **t-BUT** with hydrogen bonding shown in blue. Both **2-PROP** and **t-BUT** are included.

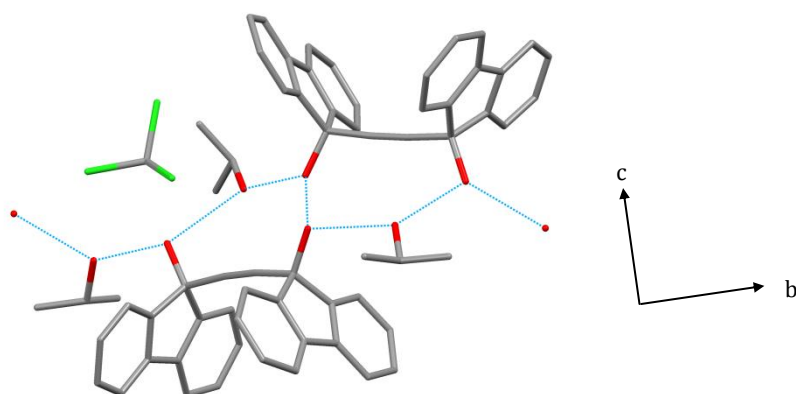


Figure 5.2: Structure **5**, grown from **2-PROP** and CHCl_3 at -20°C with hydrogen bonding shown in blue.

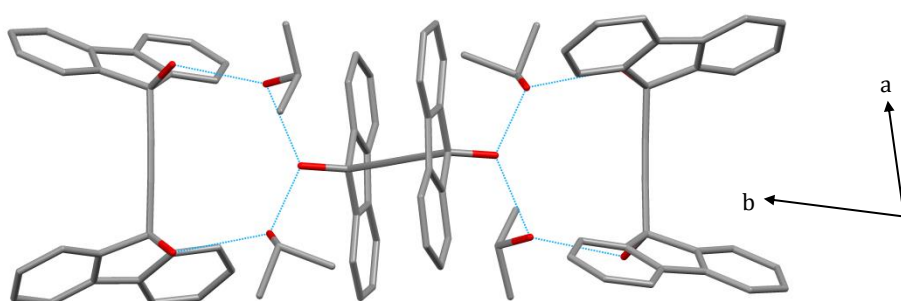


Figure 5.3: Structure **6**, grown from **2-PROP** only at -20°C, with hydrogen bonding shown in blue.

6. Apohost Composition

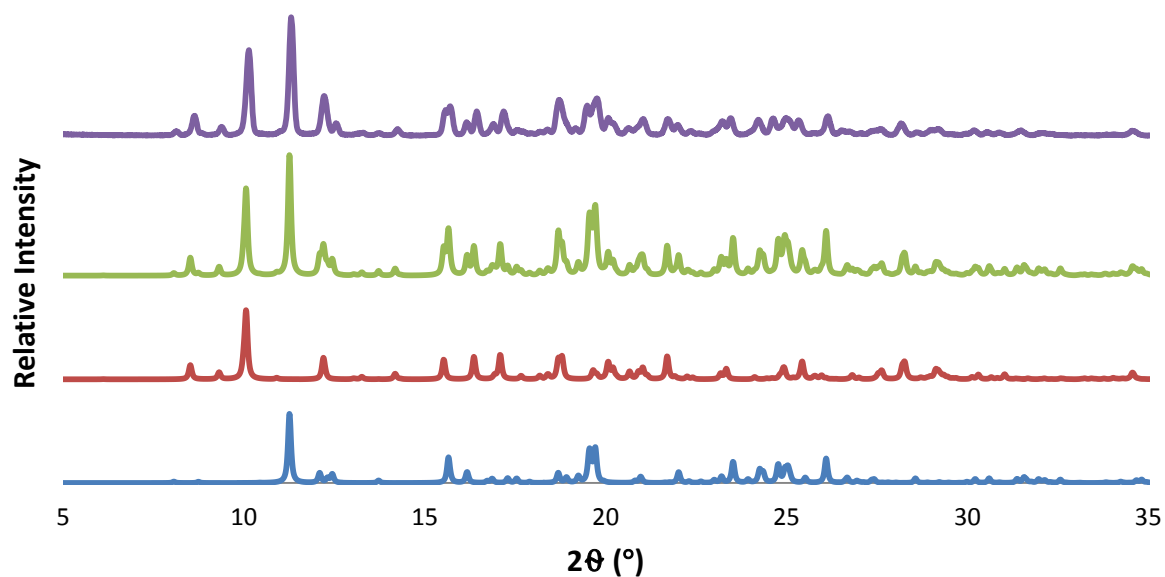


Figure 6: Structure PXRD patterns of apohost (α) (blue), apohost (β) (red) and the experimental host compound from the vial, after being sieved through $106\mu\text{m}$ (purple). The green pattern is artificially created by summing the intensities of apohost (α) and apohost (β) in a ratio of 58:42.

7. Packing comparisons between structures 1,3 and 6

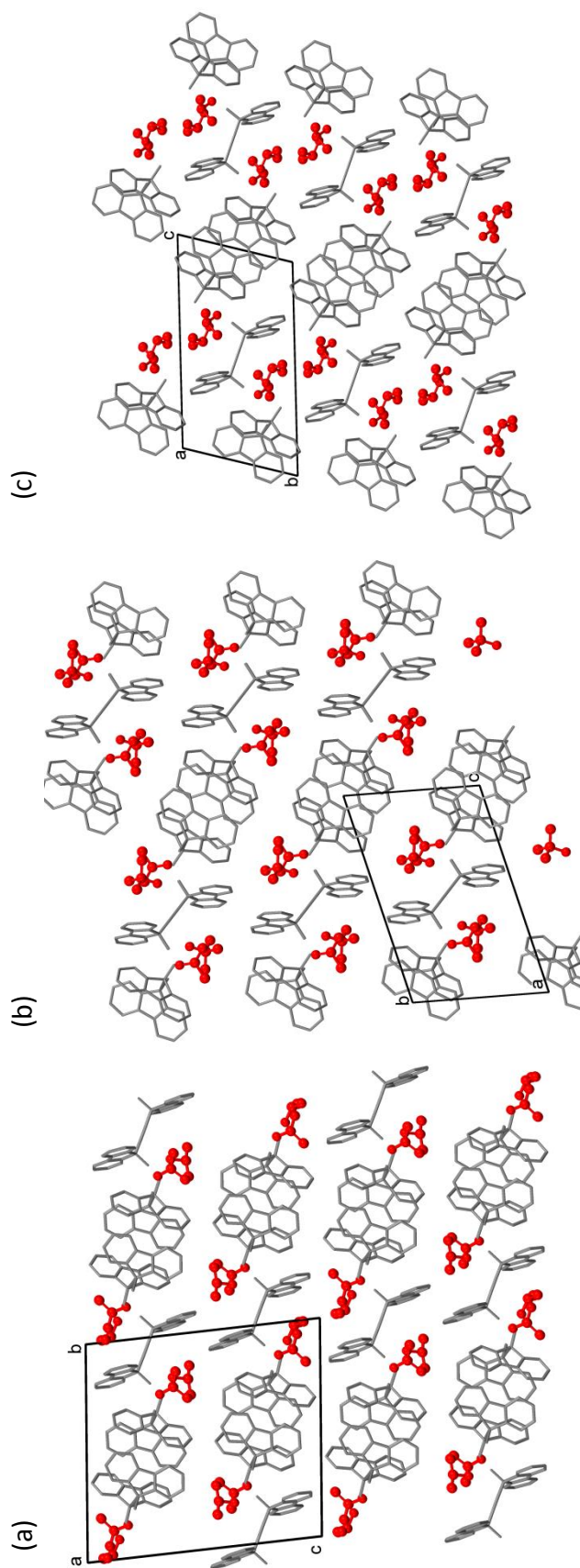


Figure 7: Structure Packing diagrams viewed down comparable directions show strong resemblances between (a) Structure 1, (b) Structure 3 and (c) Structure 6

8. Lattice Energy

We also computed the lattice energies of the various compounds by employing Gavezzotti's programme AA-CLP.^{13,14} There are several problems with the calculated lattice energies firstly because the structures are not isomeric and secondly because some of the guest molecules suffer from disorder, and Professor Gavezzotti states that such results are strictly invalid.

However, we normalised the stoichiometries to that of structure 2. What is relevant is that structure 2 (phase II) yielded $-357.0 \text{ kJ}\cdot\text{mol}^{-1}$ while structure 3 (phase I) gave $-341.6 \text{ kJ}\cdot\text{mol}^{-1}$, a difference of $15.4 \text{ kJ}\cdot\text{mol}^{-1}$, which is not significant.

Table 3. Lattice Energies

Structure	Molar mass (g/mol)	Calculated Lattice Energy (kJ/mol)	Normalized Lattice Energy relative to structure 2 (kJ/mol)	Normalised $E_{\text{structure } i} - E_{\text{structure } 2}$ $i = 1-6$ (kJ/mol)
1	1399.74	-906.5	-346.3	+10.7
2	534.70g	-357.0	-357.0	0
3	1427.79	-912.1	-341.6	+15.4
4	682.94	-520.5	-407.5	-50.5
5	1072.57	-680.4	-339.2	+17.8
6	1399.74	-877.8	-335.3	+21.7

9. Representative Inclusion Experiments

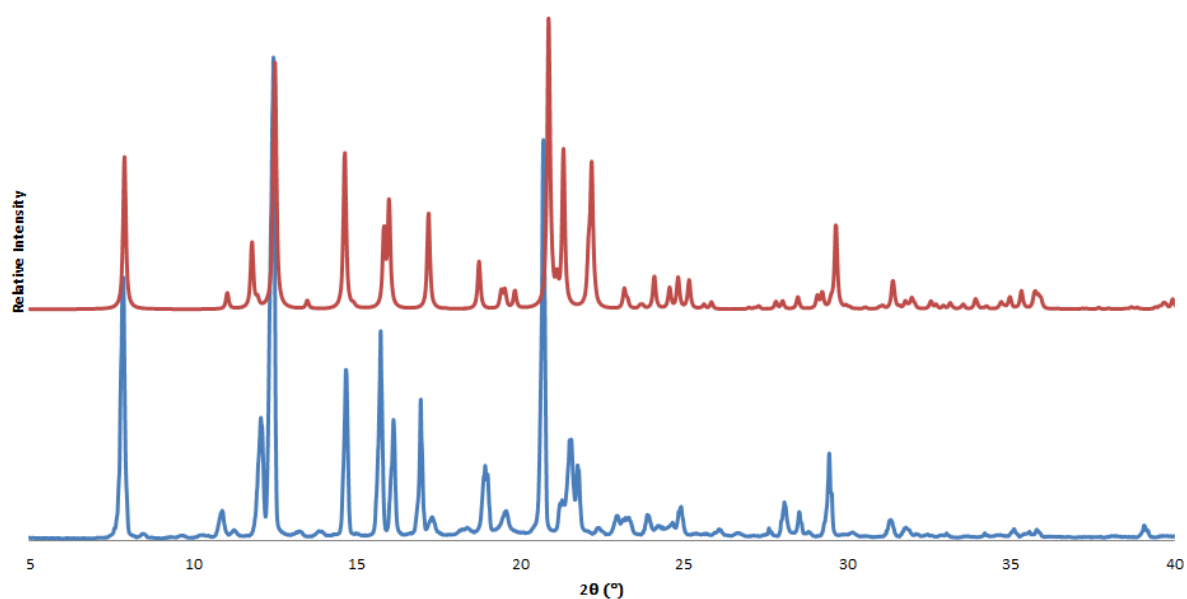


Figure 9.1. PXRD pattern of structure **2** (blue) grown from the single guest at 50°C and predicted PXRD of **2** (red)

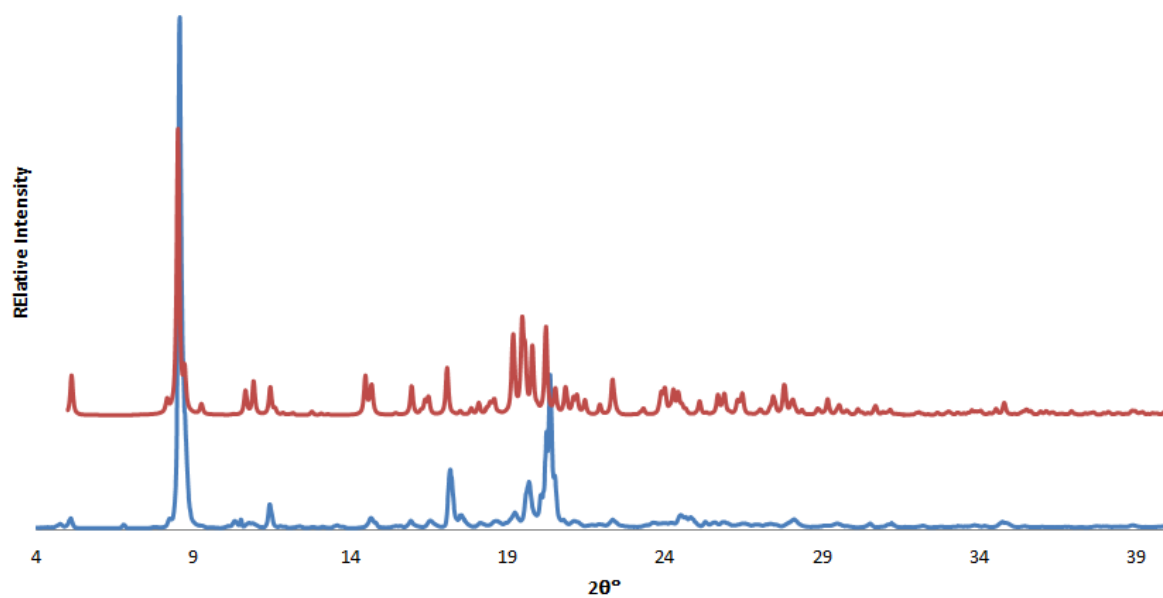


Figure 9.2. PXRD pattern of structure **1** (blue) grown from the single 2-propanol guest at 30°C and simulated PXRD pattern of **1** (red)

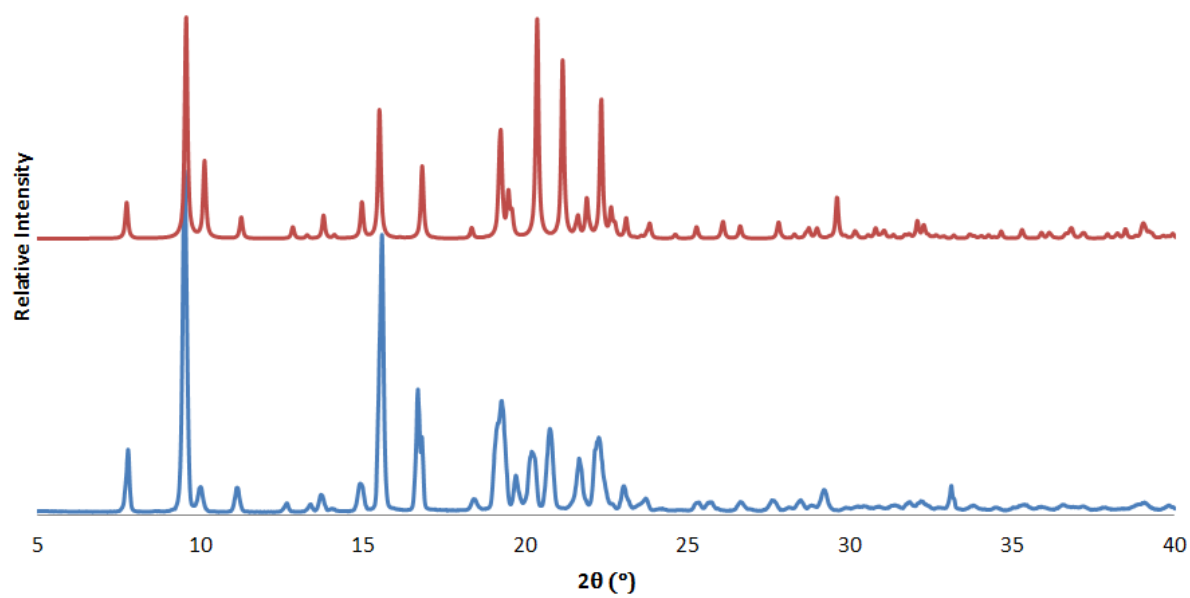


Figure 9.3. PXRD pattern of structure **4** (blue), grown from the single tertiary butanol guest at 30°C and predicted PXRD pattern of **4** (red)

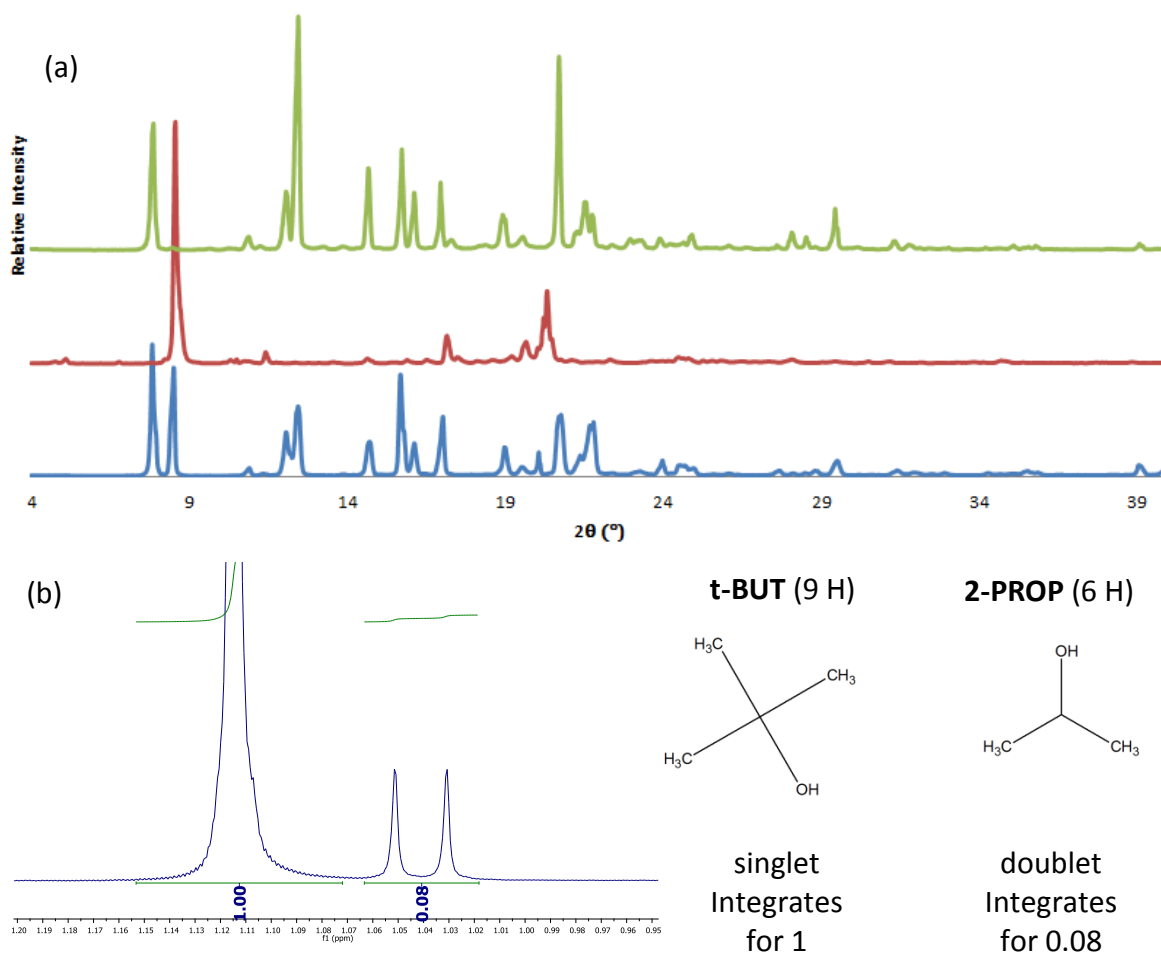


Figure 9.4. (a) PXRD pattern of the result of the equimolar competition carried out at 30°C (blue), predicted PXRD pattern of **3** (red) and PXRD pattern of **2** at 50°C (green) and (b) CH₃ region of ¹H NMR spectrum showing **t-BUT** integrating for 1 and **2-PROP** integrating for 0.08 indicating 10.7% 2-propanol in the mixture.

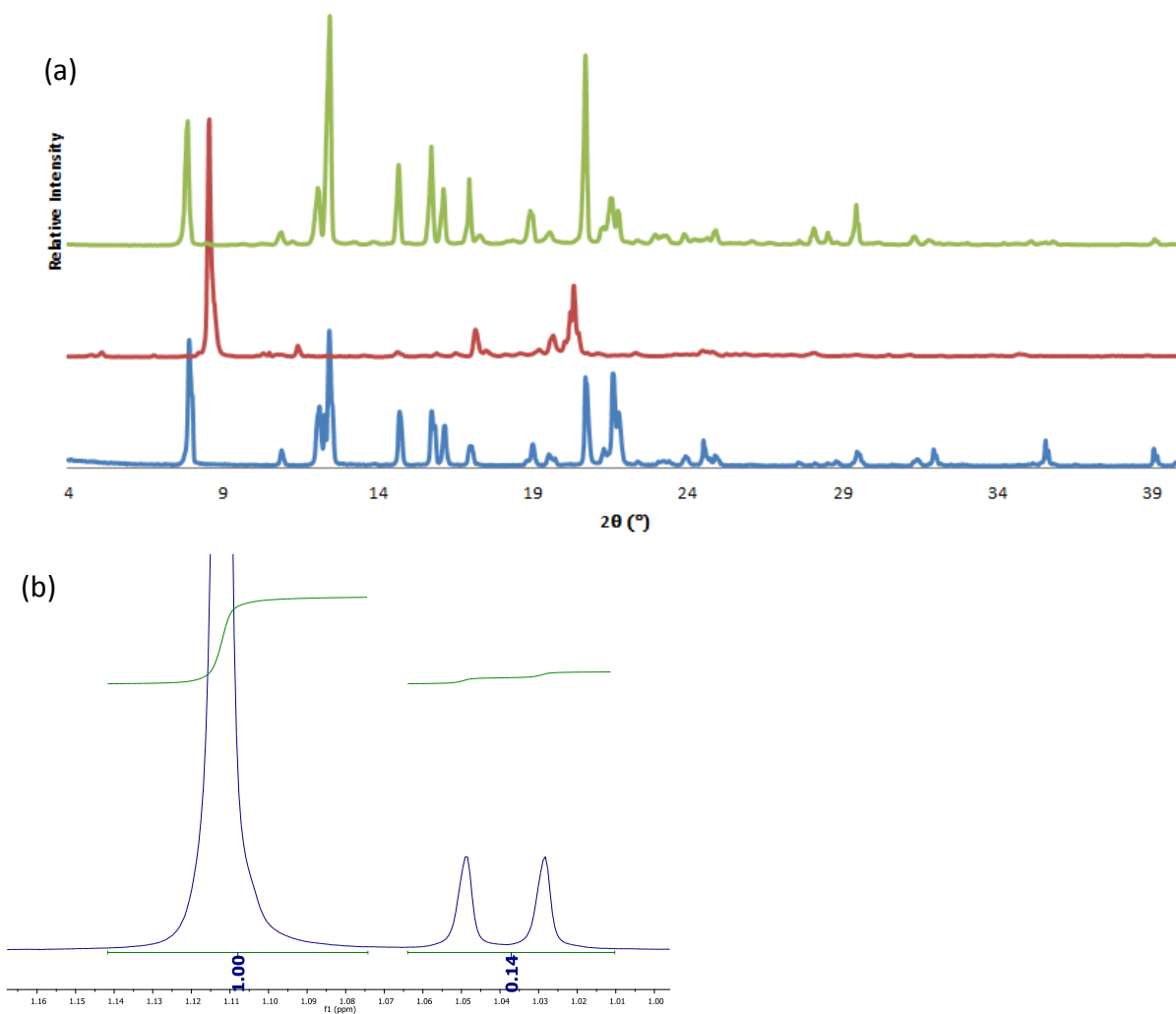


Figure 9.5. a) PXR D pattern of the result of the equimolar competition carried out at 30°C (blue), predicted PXR D pattern of **3** (red) and PXR D pattern of **2** at 50°C (green) and (b) CH₃ region of ^1H NMR spectrum showing **t-BUT** integrating for 1 and **2-PROP** integrating for 0.14 indicating 17.4% 2-propanol in the mixture.

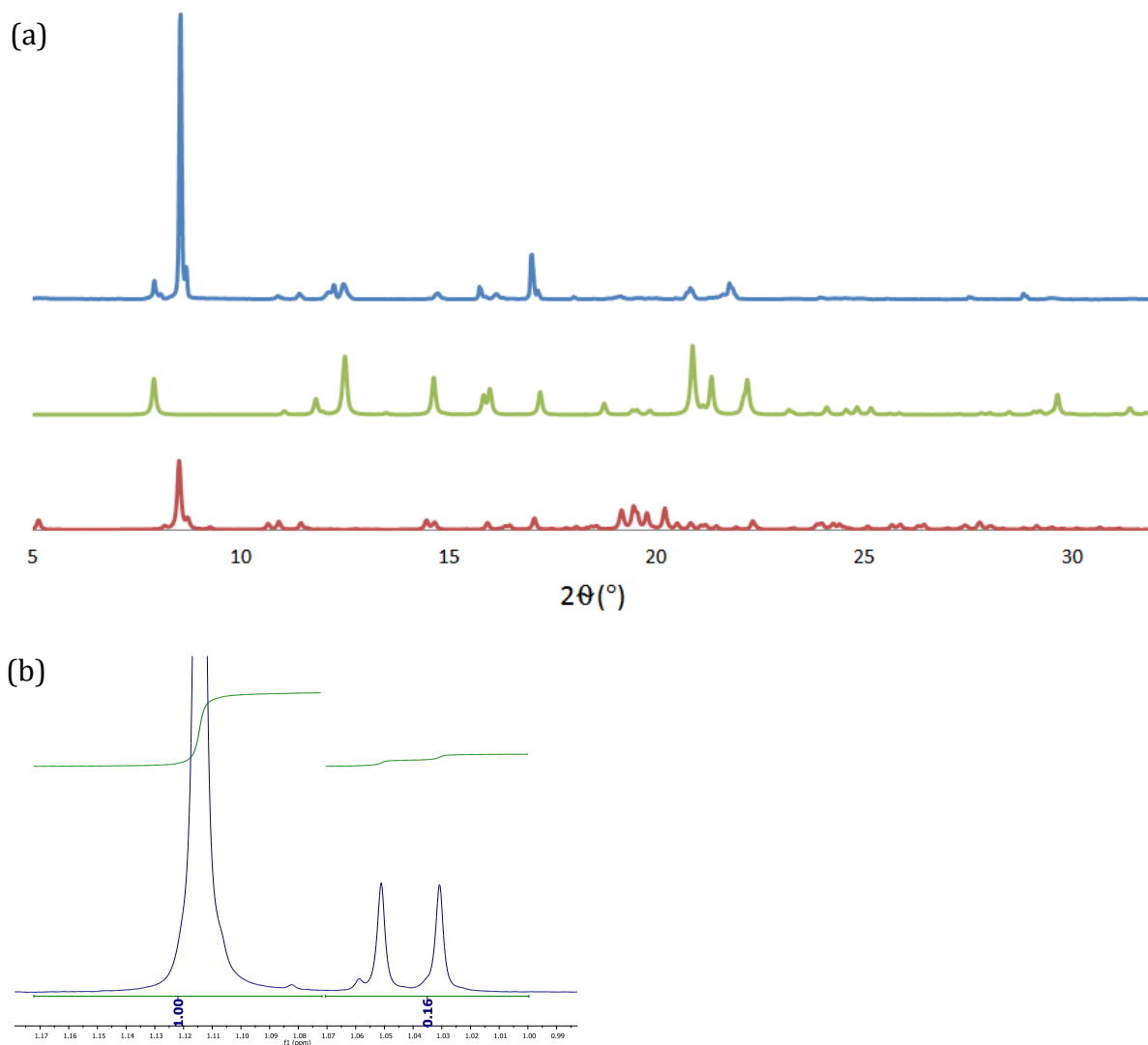


Figure 9.6. (a) PXRD pattern of the result of the equimolar competition carried out at 30°C (blue), predicted PXRD pattern of **3** (red) and PXRD pattern of **2** at 50°C (green) and (b) CH_3 region of ^1H NMR spectrum showing **t-BUT** integrating for 1 and **2-PROP** integrating for 0.016 indicating 19.4% 2-propanol in the mixture.

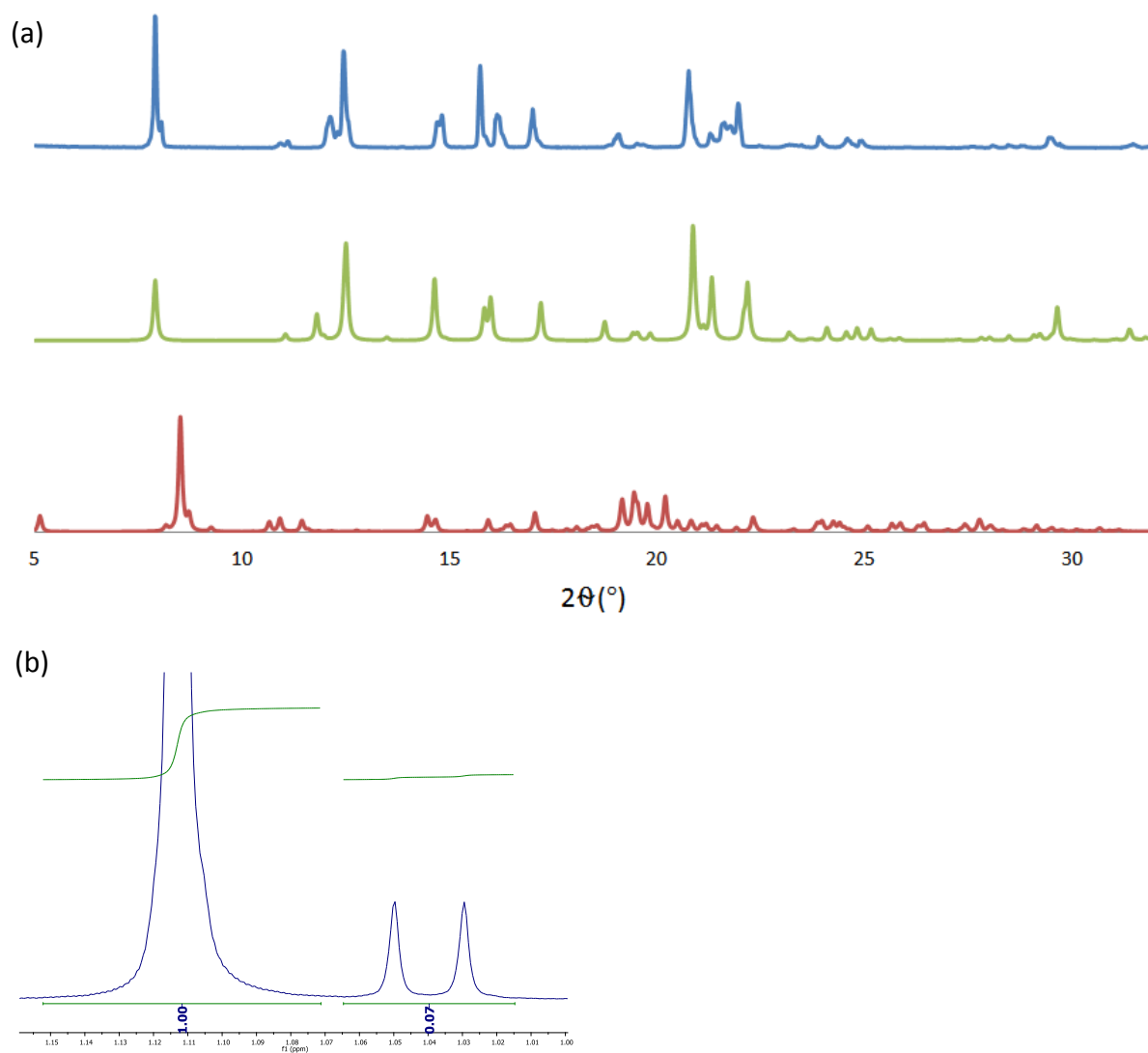


Figure 9.7. (a) PXRD pattern of the result of the equimolar competition carried out at 30°C (blue), predicted PXRD pattern of **3** (red) and PXRD pattern of **2** at 50°C (green) and (b) CH_3 region of ^1H NMR spectrum showing **t-BUT** integrating for 1 and **2-PROP** integrating for 0.07 indicating 9.5% 2-propanol in the mixture.

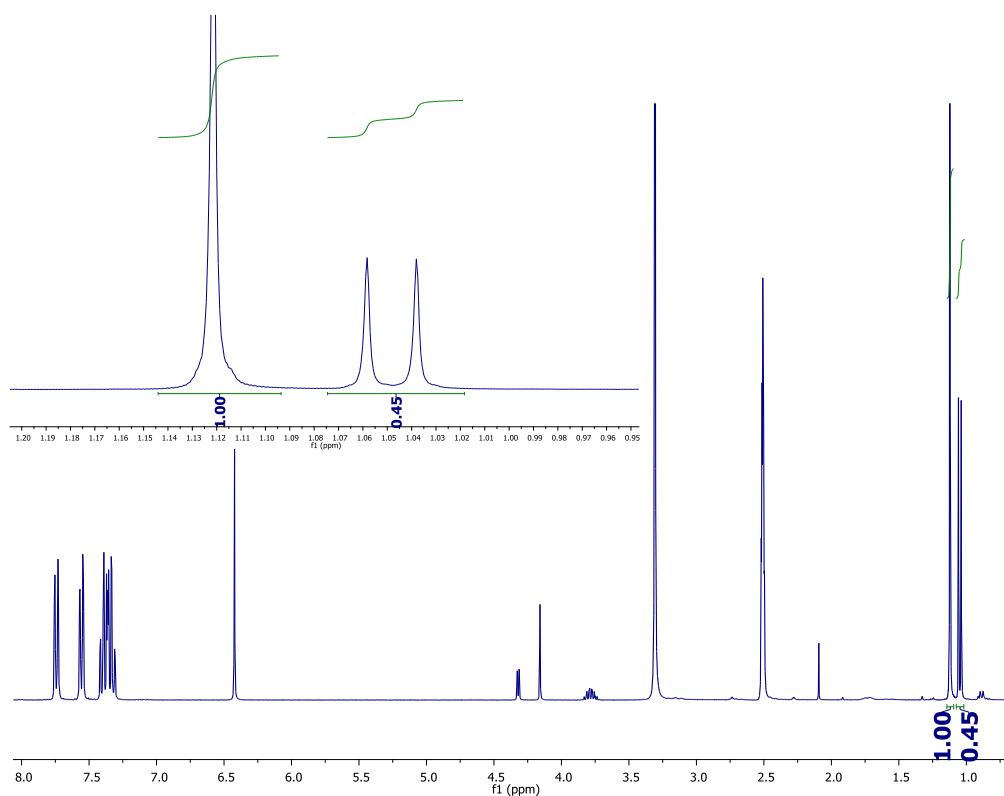


Figure 9.8. ^1H NMR spectrum of the crystals grown at 30°C from an equimolar mixture of **2-PROP** and **t-BUT** showing **t-BUT** integrating for 1 and **2-PROP** integrating for 0.45 indicating 40.3% **2-PROP** in the mixture.

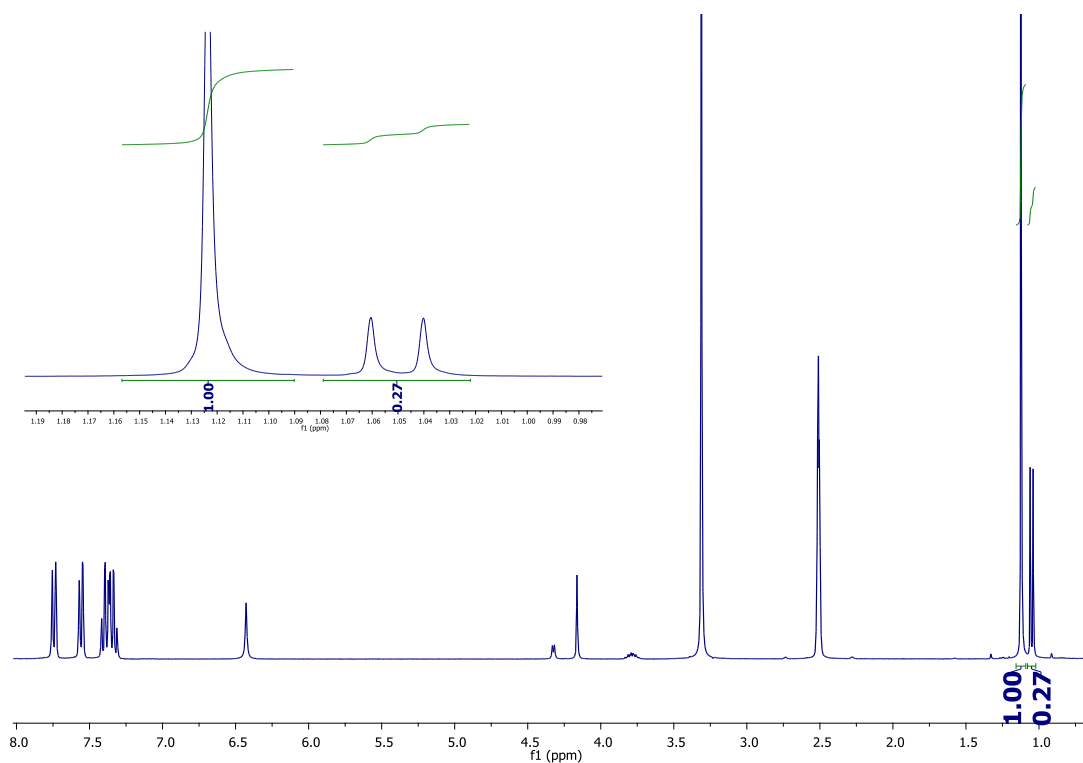


Figure 9.9: ^1H NMR spectrum of the crystals grown at 30°C from an equimolar mixture of **2-PROP** and **t-BUT** showing **t-BUT** integrating for 1 and **2-PROP** integrating for 0.27 indicating 28.8% **2-PROP** in the mixture.

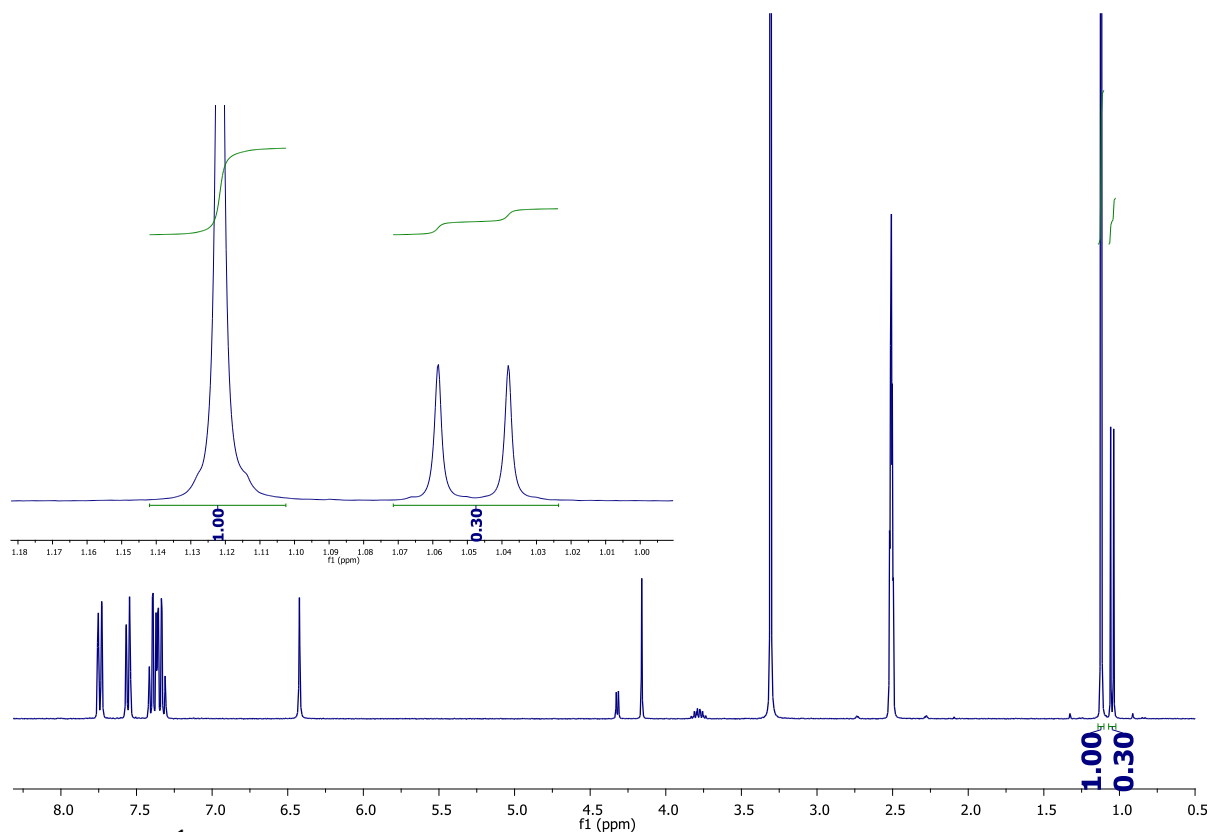


Figure 9.10. ^1H NMR spectrum of the crystals grown at 30°C from an equimolar mixture of **2-PROP** and **t-BUT** showing **t-BUT** integrating for 1 and **2-PROP** integrating for 0.30 indicating 31 % **2-PROP** in the mixture.

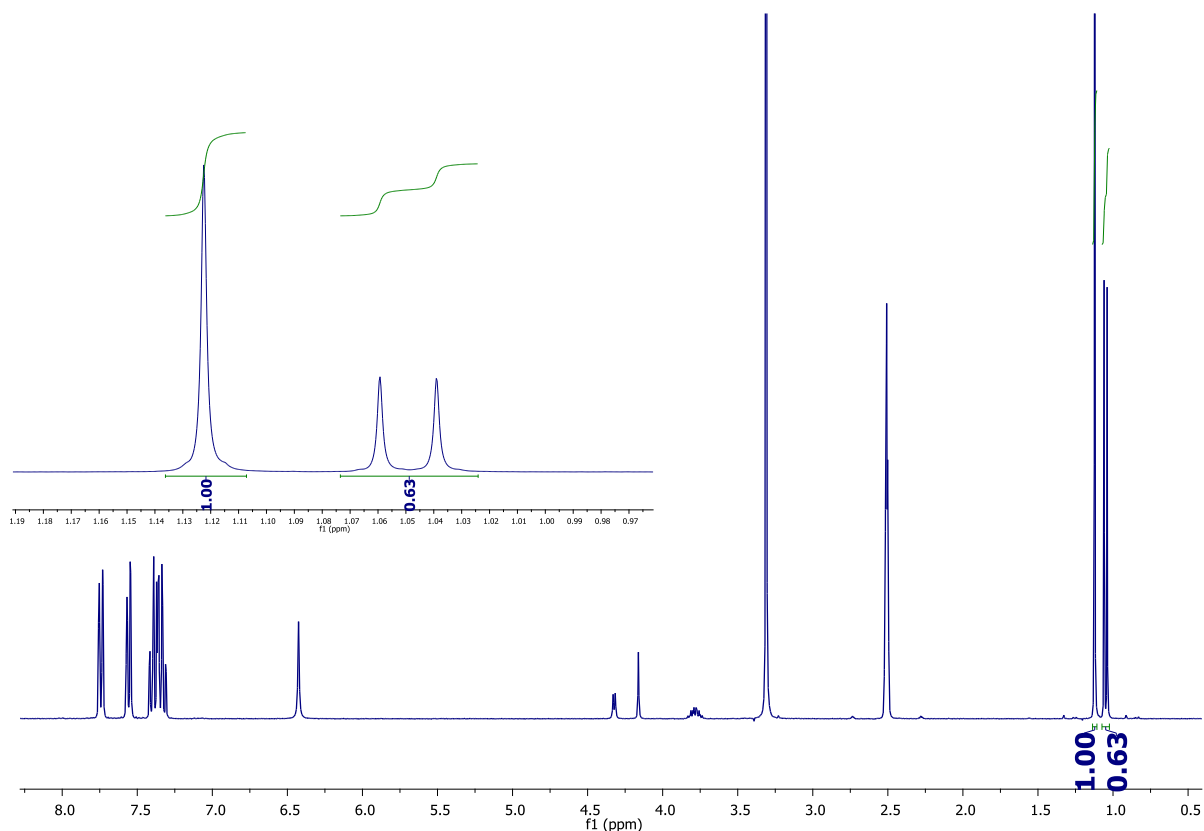


Figure 9.11. ^1H NMR spectrum of the crystals grown at 30°C from an equimolar mixture of **2-PROP** and **t-BUT** showing **t-BUT** integrating for 1 and **2-PROP** integrating for 0.63 indicating 48.6 % **2-PROP** in the mixture.

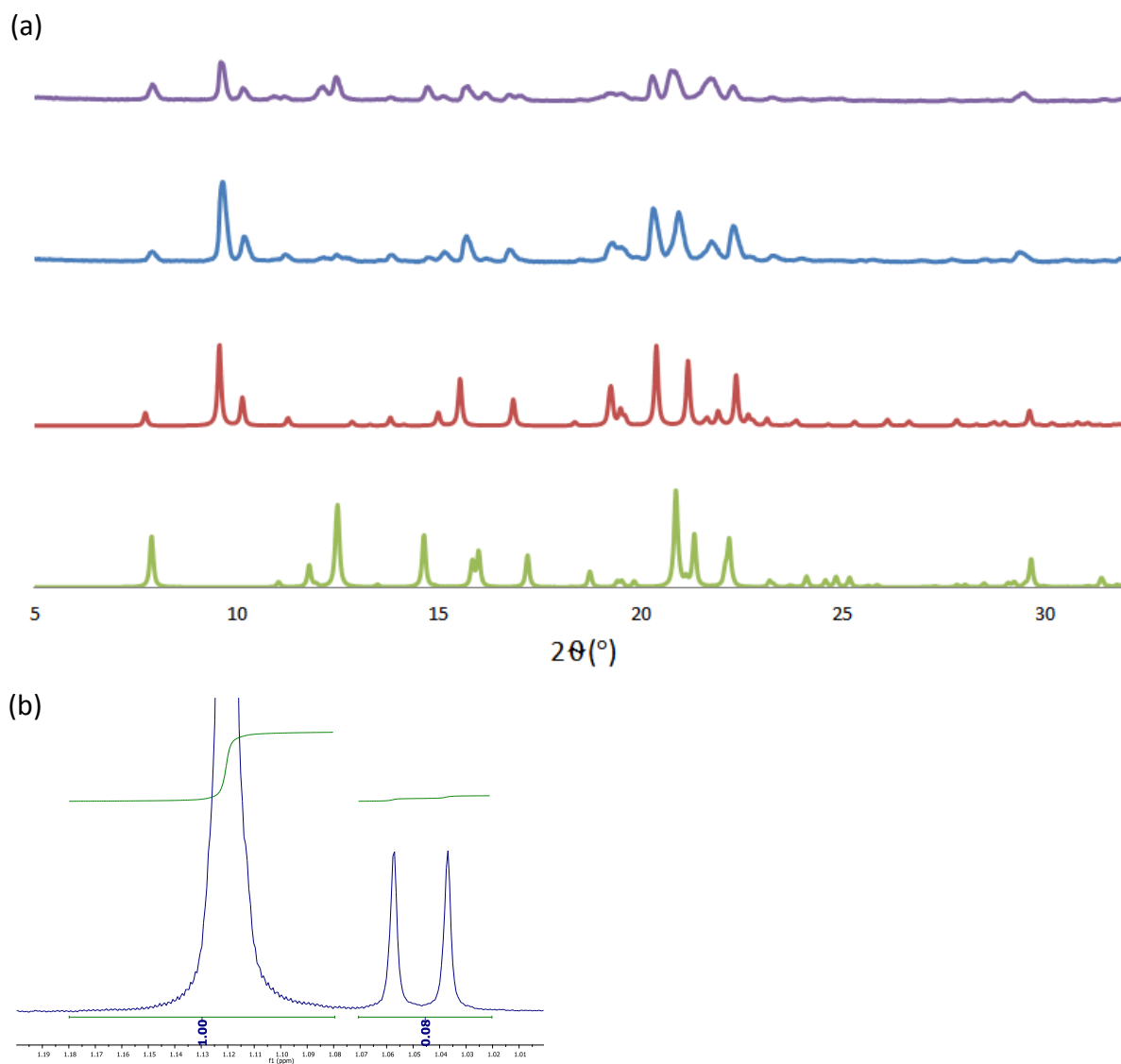


Figure 9.12. (a) PXRD pattern of the result of the equimolar competition carried out at -61°C . The blue trace is the resulting powder diffractogram and the purple trace is the diffractogram collected immediately afterwards. This is compared to the predicted PXRD pattern of **2** (green) and predicted PXRD pattern of **3** (red) and (b) CH_3 region of ^1H NMR spectrum showing **t-BUT** integrating for 1 and **2-PROP** integrating for 0.08 indicating 10.7% **2-PROP** in the mixture.

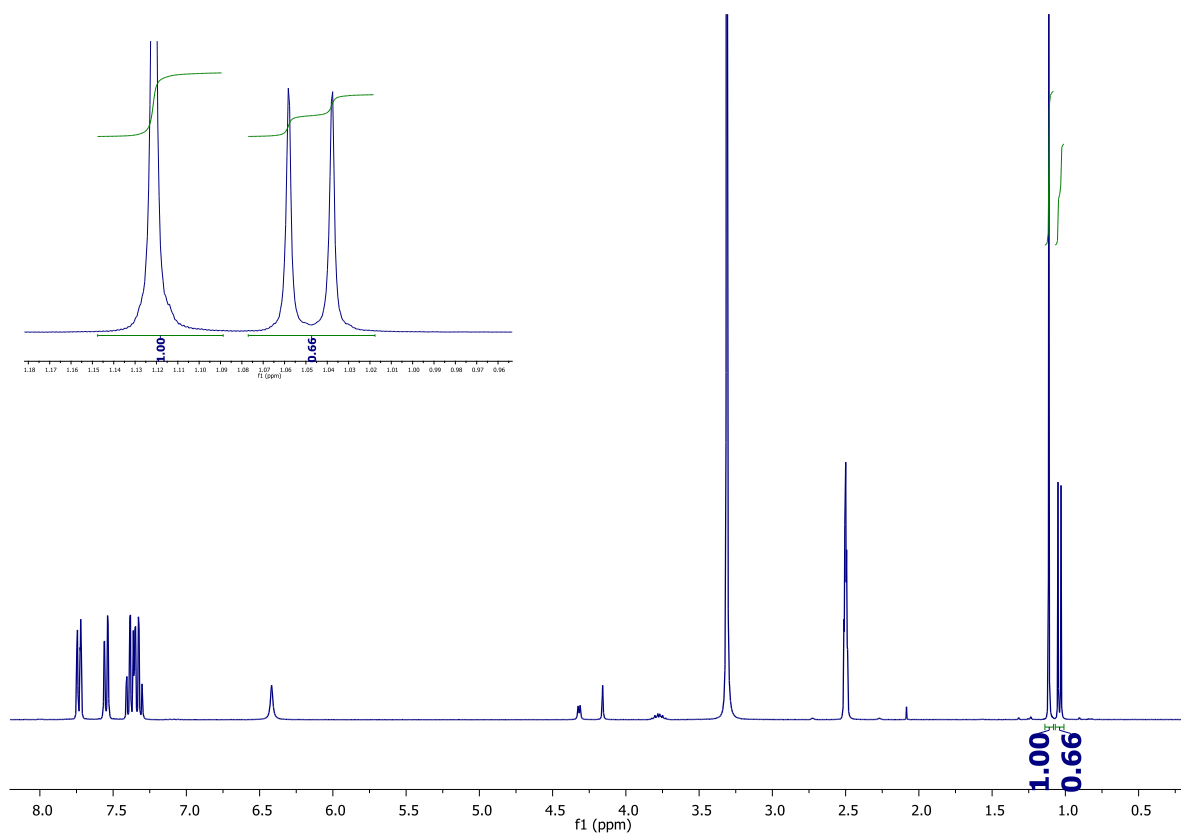


Figure 9.13. ^1H NMR spectrum of the crystals grown at 50°C from an equimolar mixture of **2-PROP** and **t-BUT** showing **t-BUT** integrating for 1 and **2-PROP** integrating for 0.66 indicating 49.7% **2-PROP** in the mixture.

10. Hirshfeld Analysis

We studied the packing of all the structures using the programme Crystal Explorer.¹² In each case we targeted the host molecule and analysed the non-bonded interactions, but the only significant differences were those between the *cis*- versus the *trans*- host molecules. This was expected and yielded no fresh insights into the mechanism of selectivity.

Hosts selected as target in all cases:

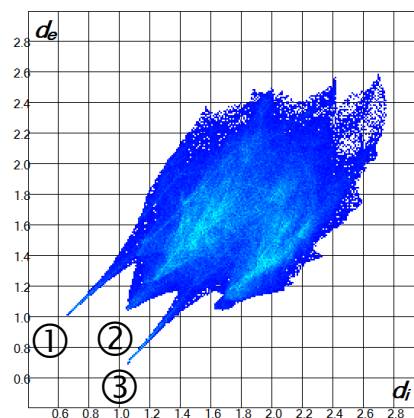
Structure 1

trans-

	Out %		
In %	C	H	O
C	0.2	26.5	0.3
H	3.3	59.8	5.4
O	0.2	4.4	0

$d_i + d_e$

- ① 1.632
- ② 2.092
- ③ 1.757

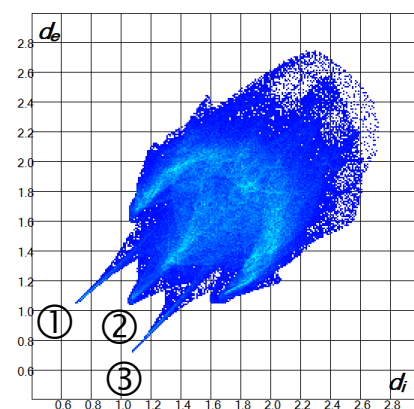


cis α -

	Out %		
In %	C	H	O
C	4.2	22.5	0.6
H	19.2	45.1	3.4
O	0.2	4.7	0

$d_i + d_e$

- ① 1.747
- ② 2.097
- ③ 1.787

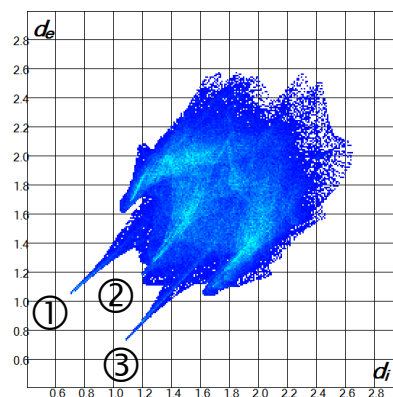


cis β -

	Out %		
In %	C	H	O
C	4.4	22.6	0.2
H	20.4	44.1	3.3
O	0.3	4.7	0

$d_i + d_e$

- ① 1.752
- ② 2.313
- ③ 1.807

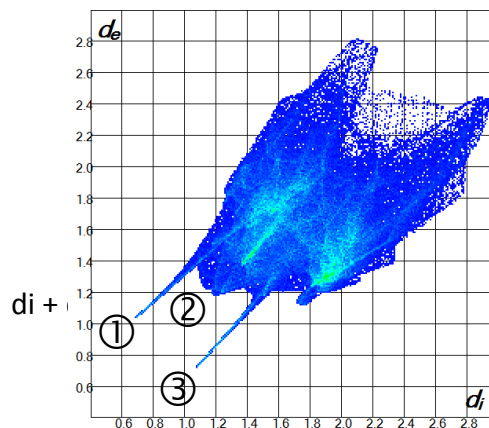


Structure 2

trans-

	Out %		
In %	C	H	O
C	0	26.7	0
H	5.8	59.4	4.0
O	0	4.2	0

- ① 1.732
- ② 2.369
- ③ 1.792



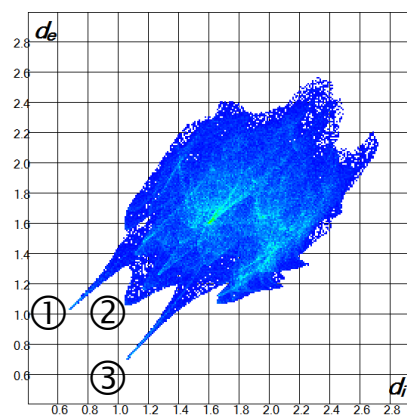
Structure 3 (major component of disordered guest selected only)

trans-

	Out %		
In %	C	H	O
C	0.3	26.2	0.3
H	5.8	57.3	5.3
O	0.2	4.5	0

$d_i + d_e$

- ① 1.697
- ② 2.098
- ③ 1.752

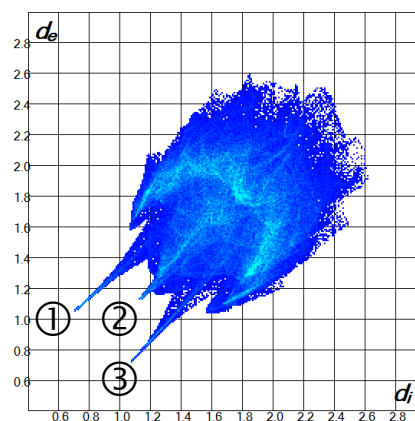


cis-

	Out %		
In %	C	H	O
C	4.1	22.5	0.2
H	19.8	45.1	3.4
O	0.1	4.8	0

$d_i + d_e$

- ① 1.747
- ② 2.239
- ③ 1.793



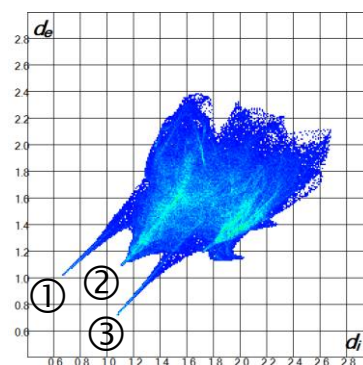
Structure 4

trans-

	Out %		
In %	C	H	O
C	0	26.1	0.5
H	3.1	62.6	3.1
O	0	4.6	0

$d_i + d_e$

- ① 1.682
- ② 2.189
- ③ 1.798

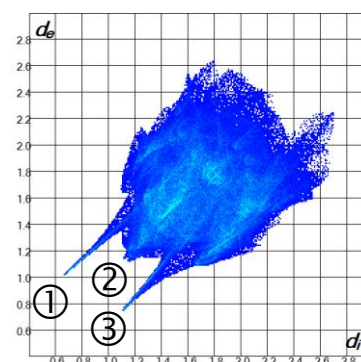


Structure 5

cis- α

	Out %			
In %	C	H	O	Cl
C	2.2	24.2	0	0.4
H	9.4	52.2	4.5	2.0
O	0	5.0	0	0

- ① 1.677
- ② 2.257
- ③ 1.857



cis-β

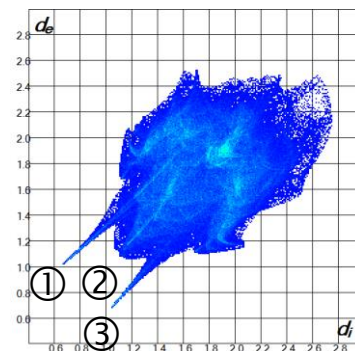
	Out %			
In %	C	H	O	CI
C	3.6	18.7	0	4.3
H	0.1	49.7	4.1	5.6
O	0	4.8	0	0.2

$d_i + d_e$

① 1.677

② 2.187

③ 1.732



Structure 6 (major component of disordered guests selected only)

trans-

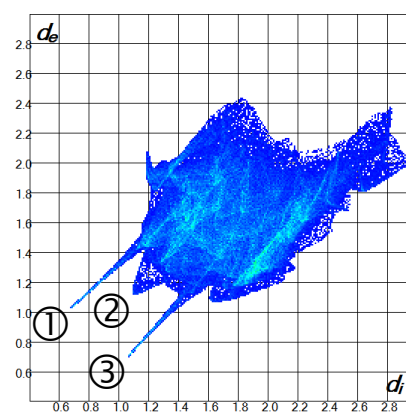
	Out %		
In %	C	H	O
C	0	27.5	0
H	5.3	53.5	8.3
O	0	5.3	0

$d_i + d_e$

① 1.692

② 2.212

③ 1.767



cis-

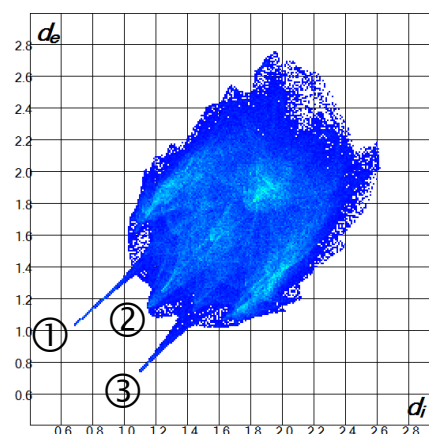
	Out %		
In %	C	H	O
C	4.4	22.8	0
H	17.7	47.0	2.8
O	0	5.2	0

$d_i + d_e$

① 1.717

② 2.267

③ 1.838



11. Kinetics of *In Situ* PXRD Vapour Sorption (Experiment 1)

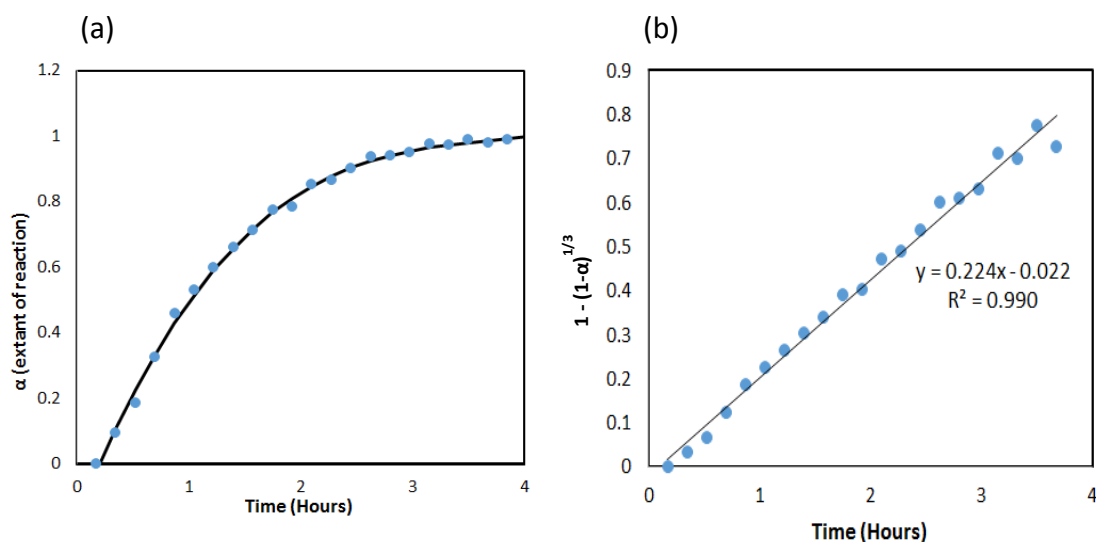


Figure 11. Experiment 1 (a) plot of extent of reaction vs time and (b) data fitted to the contracting volume equation: $1 - (1 - \alpha)^{1/3} = k t$, yielding a rate constant of $3.7 \times 10^{-3} \text{ min}^{-1}$, corresponding to a half-life of 55.4 min.

12. Relevant Thermal Analysis

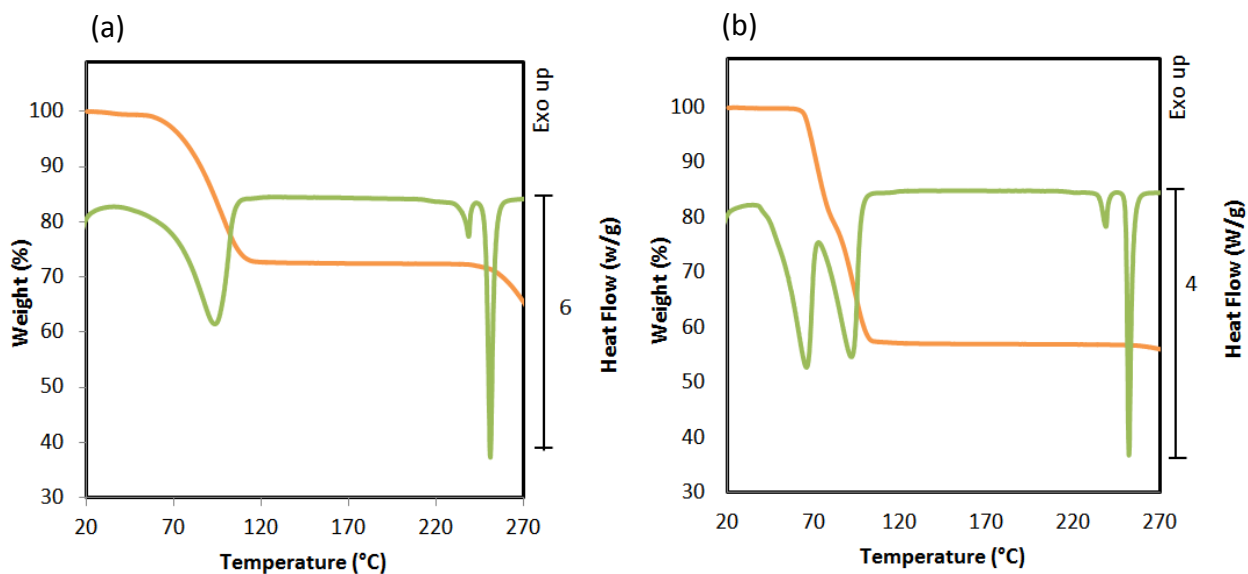


Figure 12. Thermal gravimetric (orange) and Differential Scanning Calorimetry (green) traces of (a) structure **2**, phase II (TGA: 27.5% experimental, 27.9% calculated) and (b) structure **4**, phase III (TGA: 42.9% experimental, 43.4%)